ACS OMEGA

Article

Cite This: ACS Omega 2019, 4, 20435−20442

http://pubs.acs.org/journal/acsodf

Carbohydrate Modifications of Neoandrographolide for Improved Reactive Oxygen Species-Mediated Apoptosis through Mitochondrial Pathway in Colon Cancer

Venu Sharma,*[,†] Arem Qayum,[‡] Sanjana Kaul,*[,†] Ajeet Singh,[‡] Kamal K. Kapoor,[§] Debaraj Mukherjee,[‡] Shashank K. Singh,[‡] and Manoj K. Dhar[†]

[†]School of Biotechnology and [§]Department of Chemistry, University of Jammu, Jammu 180006, Jammu & Kashmir, India

[‡]Indian Institute of Integrative Medicine, Jammu 180001, Jammu & Kashmir, India

Supporting Information

ABSTRACT: Modifications at the carbohydrate moiety of neoandrographolide, isolated from the medicinal plant *Andrographis paniculata*, result in more potent and less toxic derivatives, namely, 4′,6′-benzylidene neoandrographolide (**2b**) and 4′6′-*p*-methoxybenzylidene neoandrographolide (**2c**). These showed improved cytotoxicity against SW-620, PC-3, and A549 cancer cell lines. Nuclear morphology studies were conducted on compound **2b** by 4′,6-diamidino-2-phenylidole staining and detection of intracellular reactive oxygen species (ROS) accumulation. It showed an increase in the generation of cellular and mitochondrial ROS level. The probable relation of B-cell lymphoma-2 (Bcl-2, an apoptosis inhibitor) to B-cell lymphoma-2-associated X protein (Bax, an apoptosis promoter) ratio with caspase-3 (apoptosis coordination enzyme) in the colon cancer cell line SW-620 was investigated, and it was discovered that upon **2b** treatment, the expression of caspase-3 Bax increased remarkably. However, in **2b**-treated cells, the expression of Bcl-2 was downregulated as compared to untreated cells.

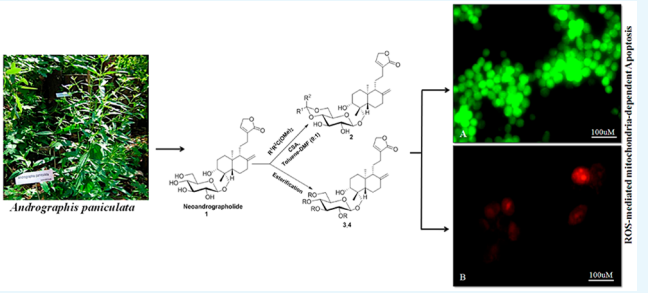

1. INTRODUCTION

Biological mechanisms in normal as well as pathogenic cells are being governed to a large extent by reactive oxygen species (ROS). These species which include superoxide ($O_2^{\bullet}$), nitroxyl radical ($NO^{\bullet}$), hydroxyl ($^{\bullet}OH$), alkoxyl ($^{\bullet}OR$), peroxyl ($ROO^{\bullet}$), and so forth act as chemical messengers and are fatal factors for DNA and proteins.[1] In normal conditions, ROS are generated through different endogenous or exogenous ways and then abolished by antioxidant systems to regulate cellular homeostasis. Strangely, mitochondria functions as a production place (mitochondrial electron transport chain) as well as a target of ROS. The sources of ROS also include xanthine oxidase, cytochrome P450, lipoxygenases, and NADPH oxidases (NOX) which are endogenous and are considered essential. In malignant cells, oxidative stress-mediated signaling phenomenon influences the cell behavior. The progression of cell cycle, cell survival and apoptosis, proliferation, cell morphology, cell motility, energy metabolism, angiogenesis, and tumor maintenance includes the involvement of ROS in neoplasm.[2] Natural products have been used as significant and potent antineoplastic entities for a long time, and carbohydrate units adjoining a natural compound change the biocompatible properties of that molecule, such as the cardiac glycoside, etoposide (glycoside of podophyllotoxin with a D-glucose derivative). It has been proved that carbohydrate modification can make a remarkable change in the activity of the bioactive molecule. Similar outcomes were observed with the glucoside modifications in the labdane diterpenoid neoandrographolide.

An ethnopharmacologically important plant, *Andrographis paniculata* (commonly known as king of bitters, *Kalmegh*,and *Chirait*), is a rich source of labdane diterpenoids,[3,4] viz., andrographolide followed by neoandrographolide and 14-deoxy-11,12-didehydroandrographolide. Although medicinal chemistry of andrographolide is well explored,[5−10] limited information is available on the semisynthetic studies of the second-principle phytoconstituent, neoandrographolide.[11] Therefore, during the present investigation, neoandrographolide was isolated from *A. paniculata* followed by the synthesis of its semisynthetic derivatives, and their cytotoxic potential was explored.

Neoandrographolide is a labdaneglucoside with molecular formula $C_{26}H_{40}O_8$, molecular mass of 480.597, and has a melting point of 165−166 °C. Its structure is a C19-*O*-*β*-D-glucopyranoside diterpene with an *α*,*β*-unsaturated lactone.[12] The biosynthesis of neoandrographolide is reported via glucosyltransferase (ApUGT)-catalyzed 19-*O*-glucosylation of andrograpanin.[13] It is soluble in methanol, ethanol, propanol,

Received: May 1, 2019
Accepted: September 4, 2019
Published: November 26, 2019

DOI: 10.1021/acsomega.9b01249
ACS Omega 2019, 4, 20435−20442

acetone, pyridine, and acetic acid. It is reported to be more a potent anti-inflammatory metabolite than andrographolide.[14] The current investigation was carried out to isolate neoandrographolide from the aerial parts of *A. paniculata* and to carry out carbohydrate modifications in it. The effect of the modified neoandrographolide was studied against different cancer cell lines. Its benzylidene derivatives **2b** and **2c** were shown to have more drug-like properties, with more potency and less toxicity than the parent molecule against the cell lines SW-620 and PC-3, respectively. Also, these compounds were found to be more biofriendly than the promising natural product andrographolide reported from the genus *Andrographis*. The molecules **2b** and **2c** were found to induce apoptosis on SW-620 cells via the mitochondria-dependent pathway mediated by ROS. In the present study, the molecules **2b** and **2c** were found to have subsided mitochondrial membrane potential and increased ROS generation in colon cancer cell lines, leading to apoptosis via the Bax-/Bcl-2-dependent apoptosis pathway. The third most common cause of neoplastic morbidity and mortality is the colon cancer. Therefore, we emphasize the execution of naturally derived biocompatible molecules on the lethal cell line SW-620.

2. RESULTS AND DISCUSSION

In the current study, 128 g (5.1%) of methanolic extract was obtained from shed, air-dried shoot plant material (2.5 kg) of *A. paniculata*. The extract was subjected to liquid−liquid partition, subsequently with hexane−methanol and dichloromethane−methanol solvents. Neoandrographolide (0.1%) was isolated as white needle-like crystals with mp 174−75 °C. It is chemically identified as *ent*-19-hydroxy-8(17),13-labdadien-16,15-olide 19-*O*-*β*-D-glucopyranoside.

The sugar residue of the isolated labdane glucoside diterpene was subjected to acetonide protection, following the method reported previously,[15] and the ester protection was done in the presence of a base (Scheme 1). 4′,6′-Diol-protected neoandrographolides were confirmed by their spectral analysis. In the ^{1}H nuclear magnetic resonance (NMR) spectrum of benzylidene derivative, a peak near δ 5.1 ppm was assigned to acetal proton, and the peak at δ 101.88 ppm in ^{13}C NMR belongs to acetal carbon. The tetraacetate derivative was characterized by four signals between δ 170.7 and 169 ppm (four acetate carbonyl carbons) in its ^{13}C NMR spectrum. In the ^{1}H NMR spectrum of the tetrabenzoate derivative, twenty aromatic protons appeared at δ 8.03−7.29 ppm as multiplets and four benzoate carbonyl carbons were displayed between 166.12 and 165.00 ppm in its ^{13}C NMR spectrum.

Scheme 1. Semisynthetic Acetal and the Ester Derivatives of Neoandrographolide

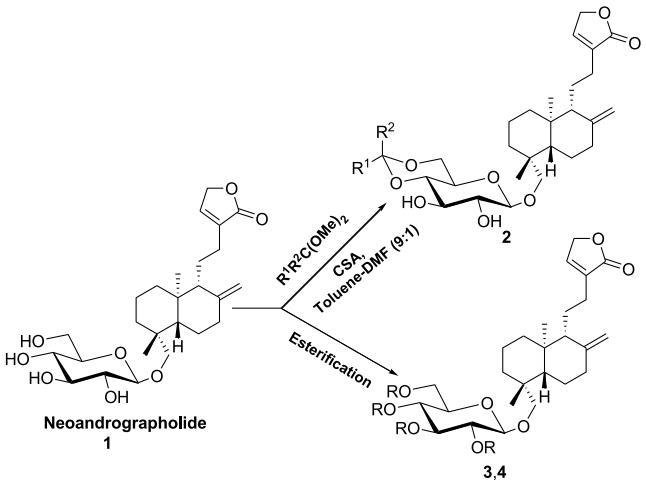

The anticancer activity of the parent compound and its derivatives was investigated against three human cancer cell lines PC-3 (prostate), SW-620 (colon), and A549 (lung) as well as in normal cell lines. Among seven molecules, two compounds, 4′,6′-benzylidene neoandrographolide (**2b**) and 4′6′-*p*-methoxybenzylidene neoandrographolide (**2c**), were found to show effective cytotoxic activity against the three human cancer cell lines. The IC_{50} value of compound **2b** against PC-3, A549, and SW-620 was 6.2, 2.65, and 1.75, respectively, and IC_{50} of compound **2c** against these three cancer cell lines was 4.65, 9.91, and 7.52, respectively (Table 1).

The ester protection of the hydroxyl groups of carbohydrate moiety does not show significant activity, whereas the acetonides were found to have good bioactivity. Compounds **2b** and **2c** (4′,6′-benzylidene neoandrographolide and 4′,6′-*p*-methoxybenzylidene neoandrographolide) were found to be more potent against the SW-620, PC-3, and A549 cell lines than the other derivatives.

In nuclear morphology study, it was observed that **2b** induced nuclear fragmentation as the concentration advanced (Figure 1). To assess the molecular mechanism of the molecule imposing apoptosis in SW-620 colon cancer cells, the mitochondrial effect of **2b** on SW-620 cells was assessed by examining the accumulation of cellular ROS. In SW-620 cells, ROS production was induced by **2b** which appeared to play a critical role in the induction of apoptotic cell death in a dose-dependent manner agreeable with the increase in concentration. ROS production was also induced by cells exposed to H_2O_2 which were used as a positive control (Figure 2).

MitoSOX Red fluorescence was used to confirm that mitochondria were crucial sites of ROS production in SW-620 cells. It recognizes superoxide synthesis to quantify mitochondrial ROS (Figure 3). It was found that an increase in the concentration of **2b** increased the production of mitochondrial superoxide. In addition, **2b** significantly inhibited mitochondrial ROS generation in SW-620 cells as compared to the positive control. These observations confirmed that **2b** plays a pivotal role in mitochondria-derived ROS-induced apoptosis. Also, with the increase in the concentration of **2b**, the antiapoptotic Bcl-2 and proapoptotic Bax protein expressions in SW-620 cells were found to be decreased and increased, respectively. Furthermore, preincubation with **2b** significantly increased the activation of caspase-3/7 compared to the control cells, which concluded an enhancement in the rate of apoptotic proteins (Figure 4).

3. EXPERIMENTAL SECTION

3.1. Instrumentation and Chemicals. The commercially available reagents were purchased from Sigma-Aldrich and solvents from SD Fine Chemicals. Melting point was measured on a Perfit melting point apparatus. The progression of reaction and purity of final products were monitored on silica gel-precoated aluminum sheets (60F254, Merck).The spots on thin-layer chromatography (TLC) plates were visualized by exposure to ultraviolet (UV) light at 254 nm, iodine vapors, and 1% cerric ammonium sulfate in water containing 30%

DOI: 10.1021/acsomega.9b01249
ACS Omega 2019, 4, 20435−20442

Table 1. Effect of Neoandrographolide and Its Derivatives on the Panels of Human Cancer Cell Lines[a]

tissue	prostate adenocarcinoma	lung adenocarcinoma	colon adenocarcinoma	normal breast epithelial
cell line	PC-3	A549	SW-620	FR-2
code	IC_{50} (μM)			
A	14 ± 0.11	15 ± 1.23	15 ± 2.11	6 ± 0.45
1	12.7 ± 0.34	5.53 ± 0.34	9.5 ± 0.89	4.2 ± 0.13
2b	6.2 ± 0.21	2.65 ± 0.78	1.75 ± 0.33	11.2 ± 0.67
2c	4.65 ± 0.45	9.91 ± 0.22	7.52 ± 0.56	10 ± 1.21
3	30.24 ± 0.02	>100	>50	32 ± 0.027
4	>100	>50	>100	23 ± 0.05
paclitaxel	0.065 ± 0.02	<0.01 ± 0.001	0.110 ± 0.003	

[a](A): Andrographolide; (**1**): neoandrographolide; (**2b**): 4′,6′-benzylidene neoandrographolide; (**2c**): 4′,6′-*p*-methoxybenzylidene neoandrographolide; (**3**): 2′,3′,4′,6′-tetra-*O*-acetyl neoandrographolide; (**4**): 2′,3′,4′,6′-tetra-*O*-benzoyl neoandrographolide.

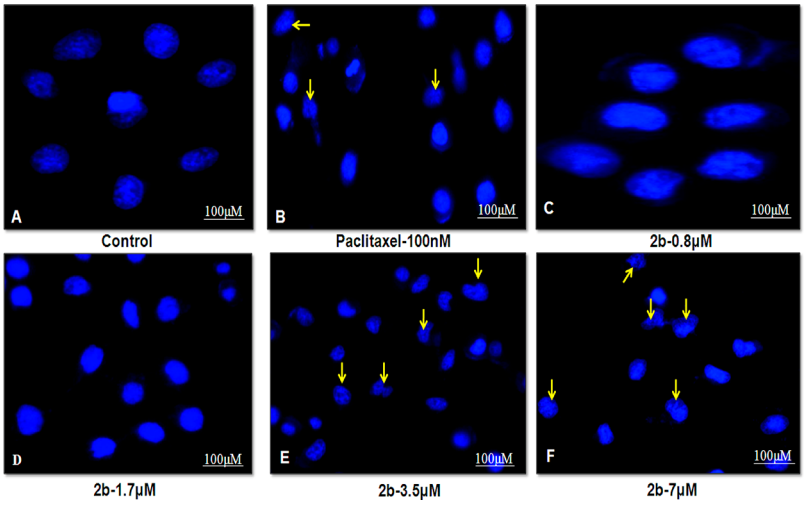

Figure 1. Nuclear fragmentation was observed with membrane blebbing (E,F) at various concentrations of **2b** (C−F) compared to untreated control (A) cells that remain intact, with no blebbing and fragmentation. Paclitaxel was used as a positive control (B).

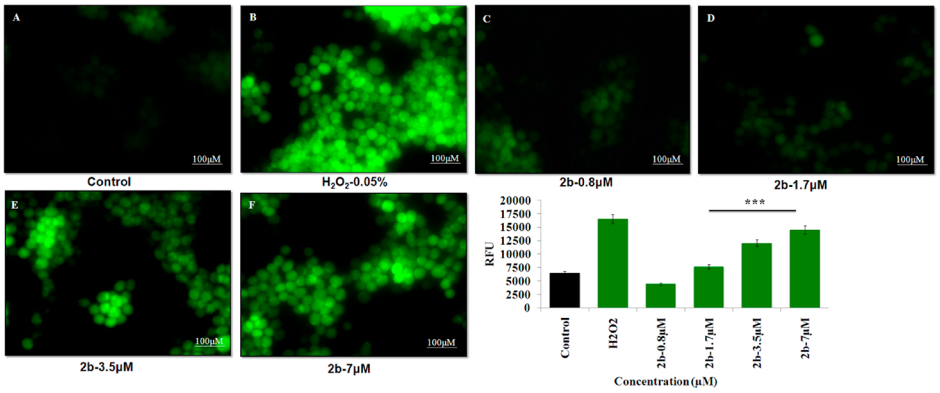

Figure 2. Generation of increased level of ROS by **2b** (E,F) in a concentration-dependent manner (C−F) leading to apoptosis in SW-620 cells as compared with H_2O_2 (B), a major contributor to oxidative damage, whereas no significant change of fluorescence was observed in control cells (A), indicating the selective targeting of **2b** in liberating ROS in SW-620 colon cancer cells and not in the control cells. Mean ± SD, $n = 3$,***$P < 0.001$.

H_2SO_4 (by volume). Column chromatography was executed on silica gel (60−120 mesh). IR spectra were recorded on a PerkinElmer spectrophotometer. Tetramethylsilane was used as an internal standard to record ^{1}H NMR and ^{13}C NMR spectra on a Bruker AC-400 spectrometer. Liquid chromatography/mass spectrometry (LC/MS) analysis was performed on an Agilent 6410 LC/MS−MS (Agilent Technologies, USA).

3.2. Plant Material. *A. paniculata* was procured from the experimental plots of School of Biotechnology, University of Jammu. The plant material was taxonomically identified, accessioned, and deposited in the herbarium of Department of Botany, University of Jammu, for future reference (accession number: 15796).

3.3. Preparation of Methanolic (MeOH) Extract. Fresh shoot parts (about 8 kg) of *A. paniculata* were collected, cleaned, air-dried, and crushed to powdered form (2.5 kg, 31.2%). Extraction of the powdered plant material was done in double-distilled methanol (5 L) at room temperature (RT) for

DOI: 10.1021/acsomega.9b01249
ACS Omega 2019, 4, 20435−20442

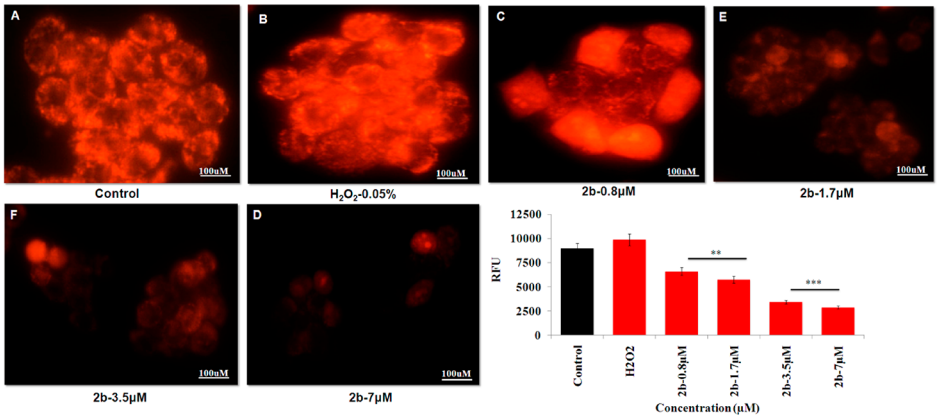

Figure 3. 2b increased mitochondrial superoxide production (A,B): SW-620 cells were incubated at the indicated concentration of **2b** and incubated with MitoSOX Red for 20 min and then analyzed by a fluorescence microscope. Significant decrease in fluorescence intensity (C−F), indicative of superoxide production, was detected in SW-620 cells compared with the control cells. Mean ± SD, $n = 3$, $^{**}P < 0.01$ $^{***}P < 0.001$.

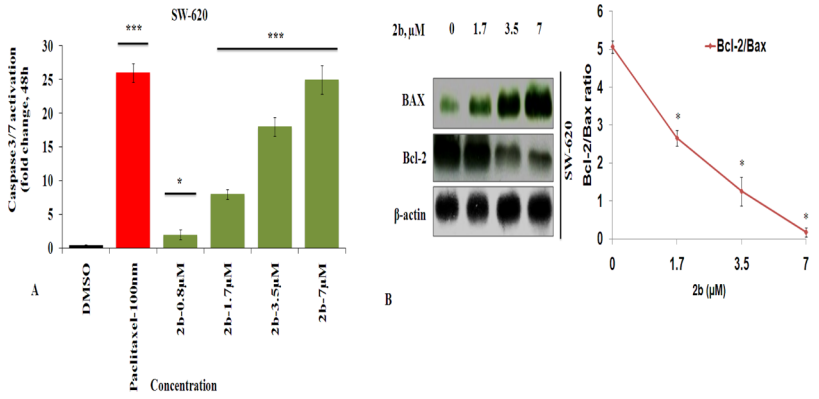

Figure 4. (A): Expression of caspase-3 protein in SW-620 cells treated with **2b** at indicated concentrations for 48 h. The treated samples showed significantly increased caspase 3/7 activity compared to the untreated one (control). Mean ± SD, $n = 3$, $^{*}P < 0.05$ $^{***}P < 0.001$. The data were analyzed by one-way analysis of variance. (B) Effect of **2b** on the expression of Bax and Bcl-2 proteins in SW-620 cells for 48 h. Mean ± SD, $n = 3$, $^{*}P < 0.05$.

Scheme 2. 1,3-Diol Protection of Neoandrographolide: (a) 2,2-Dimethoxypropane (0.12 mmol)/(b) Benzaldehyde Dimethyl Acetal (0.12 mmol)/(c) *p*-Methoxybenzaldehyde Dimethyl Acetal (0.12 mmol), RT

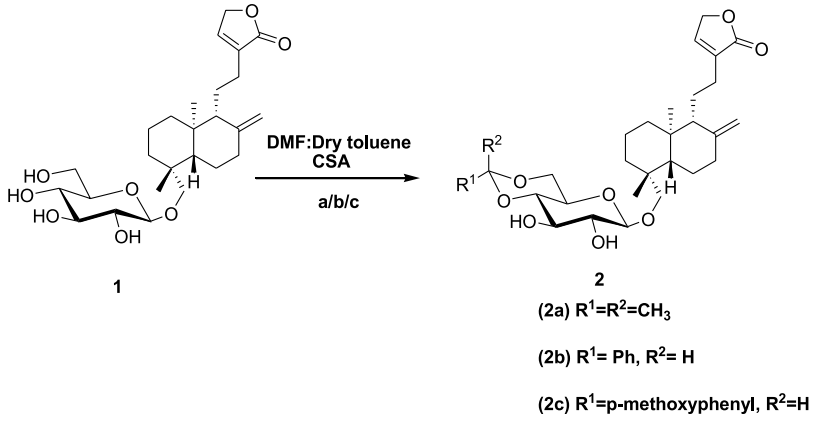

24 h, filtered, and evaporated under a reduced pressure (Buchi Rotary Evaporator, R-210). The filtrate was evaporated and combined.

3.4. Isolation of Neoandrographolide. The methanolic extract was defatted by liquid−liquid partition (three times) with hexane and methanol. After concentration, the methanol extract was extracted with dichloromethane and finally subjected to column chromatography on a 60−120 mesh silica gel using dichloromethane−methanol as the solvent system.[16] A 2.5 g (0.1%) neoandrographolide was isolated from 5% methanol in dichloromethane fraction. Colorless crystals (mp 165−166 °C) were obtained after subjecting it to crystallization in ethanol.

3.5. General Procedure for the Semisynthesis of Neoandrographolide Analogues. *3.5.1. 4′,6′-Isopropylidene Neoandrographolide (**2a**).* Neoandrographolide (48.0

DOI: 10.1021/acsomega.9b01249
ACS Omega 2019, 4, 20435−20442

Scheme 3. Acetylation of Neoandrographolide

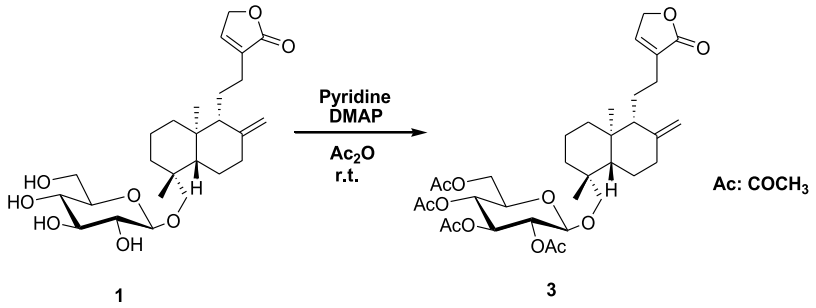

Scheme 4. Synthesis of Tetrabenzoate Neoandrographolide from Neoandrographolide

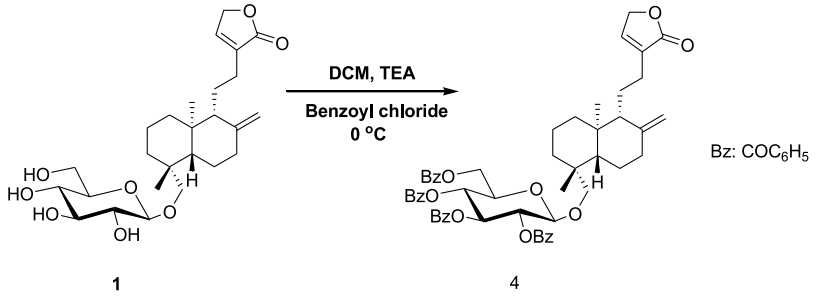

mg, 0.1 mmol), 2,2-dimethoxypropane (14.70 μL, 0.12 mmol), and camphor sulfonic acid catalyst (1.16 mg, 0,005 mmol) were dissolved in a 1:5 mixture of dry dimethylformamide and dry toluene. The reaction was carried out under a nitrogen atmosphere at RT. The progress of the reaction was monitored over TLC. After the completion of the reaction (4 h), toluene was evaporated on a rotary evaporator and the content was diluted with ethyl acetate (15 mL). The reaction mixture was treated with a saturated sodium bicarbonate solution (5 mL) and water (5 mL) to quench the remaining catalyst and was then extracted with ethyl acetate (10 mL × 3). The organic layers were collected followed by drying over anhydrous sodium sulfate and were concentrated on the rotary evaporator. The concentrated mass obtained was subjected to column chromatography over silica (60−120 mesh). Hexane/ethyl acetate (1:1) was used as an eluant to obtain 4′,6′-isopropylidene neoandrographolide with 85% yield (44 mg).

*3.5.2. 4′,6′-Benzylidene Neoandrographolide (**2b**) and 4′,6′-p-Methoxybenzylidene Neoandrographolide (**2c**).* 4′,6′-Benzylidene neoandrographolide (50.1 mg, 88% yield) and 4′,6′-*p*-methoxybenzylidene neoandrographolide (51.5 mg, 86% yield) were obtained with benzaldehyde dimethyl acetal(18 μL, 0.12 mmol) and *p*-methoxybenzaldehyde dimethyl acetal(20 μL, 0.12 mmol), respectively, using the same procedure as mentioned above (Scheme 2).[15]

*3.5.3. Tetraacetate Neoandrographolide (**3**).* Acetic anhydride (19 μL, 0.2 mmol) and a catalytic amount of dimethylaminopyridine (1.2 mg, 0.01 mmol) were added at RT[1] to neoandrographolide (48.0 mg, 0.1 mmol) in pyridine (9.66 μL, 0.12 mmol).[17] After the completion (3−4 h) of the reaction, which was checked using TLC, it was extracted with ethyl acetate. Pyridine was quenched with $CuSO_4$ solution. The resultant, after column chromatography over silica (60−120 mesh), yielded tetraacetate neoandrographolide with a yield of 76% using the solvent system hexane:ethyl acetate (7:3) as the eluent (Scheme 3).

*3.5.4. Tetrabenzoate Neoandrographolide (**4**).* For benzoylation reaction,[18] benzoyl chloride (55.8 μL, 0.48 mmol) was added dropwise at 0 °C to a stirred solution of neoandrographolide (48.0 mg, 0.1 mmol) in 1 mL dichloromethane and triethylamine (67 μL, 0.48 mmol). After the completion (3−4 h) of the reaction, it was concentrated under reduced pressure. Tetrabenzoate neoandrographolide was yielded (yield 68%) from the resultant, after column chromatography over silica (60−120 mesh), using the solvent system hexane:ethylacetate (6:4) as the eluant (Scheme 4).

3.6. Spectral Analysis. *3.6.1. Neoandrographolide (**1**).* $C_{26}H_{40}O_8$ mol. wt 480.59 amu, mp 174−75 °C, elemental analysis: observed: C, 64.08; H, 8.11; calcd: C, 64.98; H, 8.39; IR (KBr) ν_{max}: 3385, 2920, 2850, 1745, 1650, 1453, 1072 cm^{-1}; ^1H NMR (400 MHz, CD_3OD): δ 7.36 (m, 1H), 4.84 (m, 2H),4.86−4.64 (m, 2H), 4.19−4.12 (m, 3H), 3.87−3.69 (m, 2H), 3.33−3.28 (m, 2H), 3.23−3.18 (m, 2H), 1.27 (m, 2H), 1.08 (m, 2H), 2.17−2.07 (m, 1H), 1.97−1.89 (m, 3H), 1.85−1.75 (m, 3H), 1.65 (m, 3H), 1.47 (m, 2H), 1.43−1.38 (m, 1H), 1.36 (d, J = 3.9 Hz, 1H), 1.33−1.24 (m, 1H), 1.15−1.09 (m, 1H), 1.05 (s, 3H), 0.73 (s, 3H). ^{13}C NMR (100 MHz, $CDCl_3$): δ ppm 175.41, 147.8, 146.1, 133.4, 105.85, 103.6, 76.8, 76.3, 73.8, 72.2, 70.6, 70.2, 61.3, 56.3, 48.2, 47.8, 47.4, 47.7, 46.9, 39.2, 38.8, 38.2, 26.9, 24.1, 21.5, 14.4.

*3.6.2. 4′,6′-Isopropylidene Neoandrographolide (**2a**).* $C_{29}H_{44}O_8$ mol. wt 520.65 amu, mp 193−194 °C, elemental analysis: observed: C, 65.82; H, 8.17; calcd: C, 66.90; H, 8.52. Colorless crystals (85% yield). IR (KBr) ν_{max}: 3373, 2922, 2852, 1742, 1457, 1377, 1260, 1021 cm^{-1}; ^1H NMR (400 MHz, $CDCl_3$): δ 7.11 (m, 1H), 4.86 (m, 1H), 4.78−4.59 (m, 2H), 4.32−4.17 (m, 2H), 4.01 (m, 2H), 3.95−3.89 (m, 2H), 3.79 (m, 2H), 3.64−3.58 (m, 2H), 3.49−3.35 (m, 2H), 3.28−3.22 (m, 2H), 3.19 (m, 3H), 2.44−2.08 (m, 4H), 2.08 (s, 1H), 1.76−1.58 (m, 3H), 1.51 (s, 3H), 1.43 (s, 3H), 1.24 (s, 3H), 1.17−1.06 (m, 2H), 1.00 (s, 3H), 0.66−0.57 (m, 1H). ^{13}C NMR (100 MHz, $CDCl_3$): δ ppm: 171.2, 147.3, 143.8, 134.8, 106.9, 103.7, 99.7, 74.9, 72.5, 70.8, 67.3, 66.8, 64.3, 62.0, 56.0,

DOI: 10.1021/acsomega.9b01249
ACS Omega 2019, 4, 20435−20442

52.1, 49.5, 48.3, 47.8, 47.1, 46.3, 41.3, 38.2, 37.8, 32.2, 28.9, 26.5, 23.5, 14.6.

*3.6.3. 4′,6′-Benzylidene Neoandrographolide (**2b**).* $C_{33}H_{44}O_8$ mol. wt 568.69 amu, mp 142−143 °C, elemental analysis: observed: C, 69.70; H, 7.83; calcd: C, 69.69; H, 7.80; colorless solid (88% yield). IR (KBr) ν_{max}: 3384, 2923, 2856, 1740, 1707,1610, 1460, 1370, 1255, 1170, 1041, 795, 700, 667 cm^{-1}; ^1H NMR (400 MHz, $CDCl_3$): δ 8.01 (m, 1H), 7.50−7.11 (m, 5 Ar H), 5.53 (s, 1H), 4.88 (m, 1H), 4.78 (m, 2H), 4.60 (m, 1H), 4.37−4.29 (m, 2H), 4.05 (d, J = 9.4 Hz, 1H), 3.80 (dd, J = 17.3, 9.5 Hz, 2H), 3.56 (t, J = 9.3 Hz, 1H), 3.48 (d, J = 8.7 Hz, 1H), 3.43 (m, 1H), 3.23 (d, J = 9.4 Hz, 1H), 2.45 (m, 1H), 2.18−2.03 (m, 2H), 1.97−1.87 (m, 2H), 1.79 (m, 2H), 1.61 (m, 2H), 1.56 (m, 2H), 1.51−1.33 (m, 2H), 1.27−1.07 (m, 3H), 1.03 (s, 3H), 0.99−0.93 (m, 2H), 0.68 (s, 3H). ^{13}C NMR (100 MHz, $CDCl_3$): δ ppm: 174.3, 162.6, 147.3, 143.9, 137.0, 134.8, 129.2, 128.3, 126.3, 106.9, 103.7, 101.8, 80.6, 76.7, 74.8, 73.1, 72.8, 70.1, 68.7, 66.3, 56.4, 56.2, 39.5, 38.9, 38.4, 38.2, 36.5, 35.9, 27.7, 24.5, 21.7, 18.9, 15.4.

*3.6.4. 4′,6′-p-Methoxybenzylidene Neoandrographolide (**2c**).* $C_{34}H_{46}O_9$ mol. wt 598.72 amu, mp 147−148 °C, elemental analysis: observed: C, 68.18; H, 7.72; calcd: C, 68.21; H, 7.74; colorless solid (86% yield). IR (KBr) ν_{max}: 3385, 2924, 2853, 1742, 1707,1606, 1457, 1376, 1258, 1168, 1101, 1041, 794, 699, 667 cm^{-1}; ^1H NMR analysis: δ 7.43−6.90 (m, 4Ar H), 5.50 (s, 1H), 4.88 (m, 3H), 4.79 (m, 3H), 4.60 (m, 2H), 4.31 (d, J = 7.6 Hz, 1H), 4.19−3.98 (m, 4H), 3.91 (s, 3H), 3.85−3.71 (m, 4H), 3.70−3.47 (m, 3H), 3.22 (m, 4H), 2.96−2.90 (m, 4H), 2.08 (d, J = 7.0 Hz, 1 H), 1.27 (m, 3H), 1.02 (s, 3H), 0.68 (s, 3H). ^{13}C NMR (100 MHz, $CDCl_3$): δ ppm: 171.2, 162.8, 160.2, 147.3, 143.9, 134.8, 129.5, 127.6, 114.3, 113.6, 107.0, 103.7, 101.8, 80.5, 74.7, 73.1, 70.1, 66.4, 60.4, 56.4, 56.2, 55.3, 39.5, 38.4, 38.2, 27.7, 24.5, 21.7, 21.0, 20.6, 18.9, 15.4, 14.1, 1.0.

*3.6.5. Tetraacetate Neoandrographolide (**3**).* $C_{34}H_{48}O_{12}$ mol. wt 648.73 amu, mp 155−158 °C, elemental analysis: observed: C, 62.93; H, 7.44; calcd: C, 62.95; H, 7.46; colorless solid (76% yield); IR (KBr) ν_{max}: 3079, 2933, 2851, 1747, 1643, 1370, 1230, 1037, 896, 829, 755, 700, 667, 602 cm^{-1}; ^1H NMR (400 MHz, $CDCl_3$): δ 7.05 (m,, 1H), 5.20 (m, 1H), 5.08 (m, 1H), 5.00 (m, 1H), 4.85 (m, 1H), 4.79 (m, 1H), 4.60 (m, 2H), 4.39 (m, 1H), 4.28 (m,, 1H), 4.14 (m, 2H), 3.97 (d, J = 9.2 Hz, 1H), 3.68 (m, 3H), 3.18 (d, J = 9.3 Hz, 1H), 2.40 (m, 4H), 1.99 (m, 4H), 1.71 (m, 4H), 1.62 (m, 3H), 1.50 (m, 3H), 1.27 (m, 4H), 1.04 (m, 3H), 0.94 (s, 3H), 0.67 (s, 3H). ^{13}C NMR (100 MHz, $CDCl_3$): δ ppm: 174.4, 170.9, 170.7, 169.2, 143.8, 143.2, 135.6, 134.8, 121.3, 109.2, 106.8, 101.2, 80.1, 77.3, 77.0, 76.7, 71.6, 70.1, 69.6, 64.8, 61.7, 54.7, 41.3, 38.6, 38.2, 36.7, 27.6, 24.7, 23.8, 22.7, 22.7, 21.1, 20.7, 15.2.

*3.6.6. Tetrabenzoate Neoandrographolide (**4**).* $C_{54}H_{56}O_{12}$ mol. wt 897.01 amu, mp 145−147 °C, elemental analysis: observed: C, 72.28; H, 6.20; calcd: C, 72.30; H, 6.29; colorless solid (68% yield), IR (KBr) ν_{max}: 3065, 2931, 2853, 1731, 1601, 1451, 1267, 1106, 1095, 975, 853, 802, 686, 700, 667, 502 cm^{-1}; ^1H NMR (400 MHz, $CDCl_3$): δ ppm 8.03−7.29 (m, 20 Ar−H), 7.09 (m, 1H), 5.91 (t, J = 9.6 Hz, 1H), 5.66 (t, J = 9.6 Hz, 1H), 5.55 (t, J = 8.6 Hz, 1H), 4.76 (m, 2H), 4.64 (m, 1H), 4.58−4.45 (m, 1H), 4.14 (m, 1H), 4.00 (d, J = 9.2 Hz, 1H), 3.65−3.45 (m, 1H), 3.27 (d, J = 9.0 Hz, 1H), 2.51−2.33 (m, 1H), 2.17−2.03 (m, 2H), 1.84−1.65 (m, 3H), 1.53 (d, J = 14.8 Hz, 1H), 1.44 (m, 3H), 1.25 (m, 4H), 1.12 (m, 2H), 1.02−0.85 (m, 2H), 0.81 (s, 3H), 0.57 (s, 3H). ^{13}C NMR (100 MHz, $CDCl_3$): δ ppm: 174.4, 166.1, 165.8, 165.0, 147.3, 143.8, 134.8, 133.4, 133.2, 129.7, 129.6, 129.4, 129.1, 128.8, 128.7, 128.3, 126.3, 121.4, 109.3, 106.8, 106.7, 101.5, 101.2, 77.4, 77.0, 76.7, 76.7, 73.2, 72.8, 71.9, 71.7, 71.6, 70.1, 69.6, 64.8, 63.2, 61.7, 60.4, 56.4, 55.9, 47.8, 37.5, 38.9, 38.6, 39.5, 38.9, 38.3, 37.8, 36.4, 27.5, 24.6, 24.5, 21.6, 18.9, 15.1, 11.0.

3.7. Biological Screening Methodology. *3.7.1. Sulforhodamine B Assay.* The assay was performed by seeding a cell suspension of favorable cell density in 96-well flat-bottom plates (NUNC). Cell densities for each well used in the screen for SW-620-10, 000, A549-7000 and PC-3-7000, 100 μL of cell/well was plated. The cells were then incubated for 48 h and exposed to various concentrations of test materials containing a complete growth medium. Paclitaxel was used as a positive control. The plates were further incubated under the same conditions for another 48 h at 37 °C. The cells were then fixed with cold trichloroacetic acid for 1 h at 4 °C. After 1 h, the plates were rinsed three times with water and allowed to air dry. After drying, 100 μL of 0.4% sulforhodamine B (SRB) dye was added and kept for half an hour at RT. The plates were subsequently washed three times with 1% v/v acetic acid to remove the unbound SRB. After drying at RT, the bound dye was solubilized by adding 100 μL of 10 mM Tris (tris(hydroxymethyl)aminomethane) buffer (pH 10.4) to each well. To solubilize the protein-bound dye, the plates were kept on the shaker for 5 min. Finally, OD was taken at 540 nm in a microplate reader. IC_{50} values were determined by plotting OD against concentration.[19]

$$\%\ \text{of cell inhibition} = \frac{\text{absorbance of cells (treated)} - \text{absorbance of blank}}{\text{absorbance of cells (control)} - \text{absorbance of blank}} \times 100$$

$$\%\ \text{growth inhibition} = 100 - \%\ \text{cell viability}$$

3.7.2. Nuclear Morphology Assessment. Nuclear morphology study was done using the dye 4′,6-diamidino-2-phenylidole (DAPI). DAPI binds to the minor groove of double-stranded DNA, with a preference for the adenine−thymine clusters in the interphase of the mitotic cell. The formation of apoptotic bodies was confirmed by performing DAPI staining to visualize whether the cell nucleus in the fragmented form remains intact after treatment with the molecule. Human cancer cells SW-620 (colon cancer) were seeded at 1.5×10^5 cells/mL/well in six-well tissue culture plates in RPMI medium supplemented with 10% fetal bovine serum. This was followed by incubation for 24 h at 37 °C in a CO_2 incubator. After 24 h, the cells were treated with this different concentration of stock solution and with paclitaxel (positive control) and incubated for 48 h. After 48 h, the incubation medium was removed, and the cells were fixed with methanol followed by incubation for 20 min at 37 °C. After fixation, the cells were stained with DAPI (1 μg/mL) and incubated for 20 min in the dark at RT. The dye was removed and washed with 1% phosphate-buffered saline and examined under an inverted fluorescence microscope (Olympus, 1 × 81).[20]

3.7.3. Detection of Intracellular and Mitochondrial ROS Levels. Cellular and mitochondrial ROS levels were determined using DCFDA and MitoSOX Red, respectively, according to the manufacturer's instructions. Briefly, SW-620 cells (2×10^5 mL/well) were seeded in six-well tissue culture plates and incubated at 37 °C for 24 h. After 24 h, the cells were treated with **2b** at different concentrations (0.8, 1.7, 3.5,

DOI: 10.1021/acsomega.9b01249
ACS Omega 2019, 4, 20435−20442

and 7 μM) and incubated for 48 h. After this, the media were removed, and DC-FDA and MitoSOX Red dye were added and further incubated for 20 min at 37 °C. Before the addition of the dye, the cells were incubated with H_2O_2 (0.05%) as a positive control for 15 min. The total cellular and mitochondrial ROS levels were monitored by a fluorescence microscope (Olympus, 1 × 81).[21]

3.7.4. Caspase-3/7 Activity Assay. The activity of caspase-3/7 in SW-620 cell lysates was performed by using the fluorescent assay (caspase-3/7 activity assay kit #5723). It contains a fluorogenic substrate (*N*-acetyl-Asp-Glu-Val-Asp-7-amino-4-methylcoumarin or Ac-DEVD−AMC) for caspase-3/7 and cleaves this substrate between DEVD and AMC, generating a highly fluorescent AMC proportional to the number of apoptotic cells in the sample. This is detected using a fluorescence reader with excitation at 380 nm and emission between 420 and 460 nm. The SW-620 cells were seeded at 1 × 10^5 cells/well in a 96-well plate and kept overnight. After 24 h, the cells were treated with different concentrations of **2b** for 48 h and then lysed in 30 μL of lysis buffer (1×) (supplied with the kit). The cell lysate was mixed with the substrate solution, incubated at 37 °C in the dark for 2 h, and visualized using a relative fluorescent unit.[22]

3.7.5. Western Blotting Analysis. The SW-620 cells were centrifuged at 1200*g* for 10 min, and the cell pellet was collected and lysed with a lysis buffer (50 mM Tris-HCl pH 8.0, 120 mM NaCl, 0.5% NP-40, 1 mM phenylmethylsulfonyl fluoride). A 50 μg of protein was loaded onto 10% sodium dodecyl sulfate−polyacrylamide gel and electrophoresed. After electrophoresis, the protein was transferred to a polyvinylidene difluoride membrane (Millipore, IPVH00010, USA), and the membrane was blocked with 5% nonfat dry milk in tris-buffered saline-Tween buffer 7 (0.12 M Tris base, 1.5 M NaCl, 0.1% Tween 20) at RT for 2 h. The membrane was then incubated with primary mouse antibody against β-actin (1:2000), Bax (1:2000 #5023), and Bcl-2 (1:2000# 15701) (Cell Signaling Technologies) overnight at 4 °C followed by incubation with horseradish peroxidase-conjugated secondary antibody (antimouse #7076 and antirabbit #7074 1:1000) for 1 h at RT. Protein−antibody complexes were detected using chemiluminescence (Immobilon Western chemiluminescent HRP substrate, MERCK Millipore, USA).[23]

4. CONCLUSIONS

Various studies have reported that increased intracellular ROS can cause cell membrane potential damage and thus block the cell cycle, get into the cell nucleus to cause DNA damage, further activate the endogenous pathway, and ultimately lead to cell death. In the current study, neoandrographolide was isolated from *A. paniculata* to generate its hydroxyl-protected 19-*O*-β-glucoside analogues. An increase in the anticancer activity was observed in its acetonides. These derivatives were assessed for enhancement in their anticancer potential as compared to the parent molecule. 4′,6′-Benzylidene neoandrographolide inhibited the proliferation of SW-620 colon cancer cells by increasing the intracellular ROS levels, which resulted in an increased oxidative stress, and, subsequently, induced apoptosis. Taken together, 4′,6′-benzylidene neoandrographolide induced apoptosis on SW-620 cells via ROS-mediated mitochondria-dependent pathway. To find out the molecular mechanism of the active molecules, nuclear morphology studies were done by DAPI staining and intracellular ROS accumulation detection. The derivative **2b** showed an increase in the generation of cellular and mitochondrial levels of ROS in a concentration-dependent manner, ultimately leading to apoptosis. This was caused by ROS through the involvement of the mitochondrial pathway in SW-620 colon cancer cells. The inactivation of Bcl-2 is carried out by caspase−3 which acts downstream of Bax/Bcl-2, enabling its anti-apoptotic capacity to promote cell death.[24] It may be concluded that **2b** significantly induces an apoptotic effect on colorectal cancer cells in vitro, through its mechanism associated with the Bcl-2/Bax/caspase-3 pathway. To the best of our knowledge, the present study is the first report on the semisynthesis of neoandrographolide derivatives and their anticancer studies. Therefore, 4′,6′-benzylidene neoandrographolide is a novel candidate for antitumor therapy in patients with colon cancer.

■ ASSOCIATED CONTENT

Supporting Information

The Supporting Information is available free of charge at https://pubs.acs.org/doi/10.1021/acsomega.9b01249.

^{1}H NMR of neoandrographolide, ^{1}H, ^{13}C, DEPT NMR, LCMS, and HPLC profile of 4′,6′-*O*-benzylidene neoandrographolide and ^{1}H, ^{13}C NMR, LCMS, and HPLC profile of 4′,6′-*O*-(4-methoxybenzylidene) neoandrographolide (PDF)

■ AUTHOR INFORMATION

Corresponding Authors

*E-mail: venusharma80@gmail.com. Phone: 911912456534 (V.S.).

*E-mail: sanrozie@rediffmail.com (S.K.).

ORCID

Venu Sharma: 0000-0002-9830-9043

Debaraj Mukherjee: 0000-0002-2162-7465

Notes

The authors declare no competing financial interest.

■ ACKNOWLEDGMENTS

The authors would like to acknowledge Director, School of Biotechnology and Co-coordinator, Bioinformatics Centre, School of Biotechnology, University of Jammu for facilities. V.S. would like to thank the Department of Science and Technology, Government of India, for funding under WOS-A Projects [SR/WOS-A/CS-111/2013 (G) and SR/WOS-A/CS-46/2018]. Other funding agencies like the Department of Biotechnology, GOI, and the Department of Science and Technology, GOI, are also acknowledged for various facilities in the School. Dr. Harish Dutt, Assistant Professor, Department of Botany, University of Jammu, is acknowledged for identification of the plant materials.

■ REFERENCES

(1) Simon, H.-U.; Haj-Yehia, A.; Levi-Schaffer, F. Role of reactive oxygen species (ROS) in apoptosis induction. *Apoptosis* **2000**, *5*, 415−418.

(2) Liou, G. Y.; Storz, P. Detecting reactive oxygen species by immunohistochemistry. *Stress Responses*; Humana Press: New York, NY, 2015, pp 97−104.

(3) Demetzos, C.; Dimas, K. S. Labdane-type diterpenes: Chemistry and biological activity. *Stud. Nat. Prod. Chem.* **2001**, *25*, 235−292.

(4) Kenmogne, M.; Prost, E.; Harakat, D.; Jacquier, M.; Frederich, M.; Sondengam, L.; Zeches, M.; Waffoteguo, P. Five labdane

DOI: 10.1021/acsomega.9b01249
ACS Omega 2019, 4, 20435−20442

diterpenoids from the seeds of Aframomum zambesiacum. *Phytochemistry* **2006**, *67*, 433−438.
(5) Sharma, V.; Sharma, T.; Kaul, S.; Kapoor, K. K.; Dhar, M. K. Anticancer potential of labdanediterpenoid lactone "Andrographolide" and its derivatives: A semi-synthetic approach. *Phytochem. Rev.* **2017**, *16*, 513−526.
(6) Sule, A.; Ahmed, Q. U.; Samah, O. A.; Omar, M. N.; Hassan, N. M.; Kamal, Z. M.; Yarmo, M. A. Bioassay guided isolation of antibacterial compounds from *Andrographispaniculata*. *Am. J. Appl. Sci.* **2011**, *8*, 525−534.
(7) Singha, P. K.; Roy, S.; Dey, S. Antimicrobial activity of *Andrographispaniculata*. *Fitoterapia* **2003**, *74*, 692−694.
(8) Mishra, K.; Dash, A. P.; Swain, B. K.; Dey, N. Anti-malarial activities of *Andrographispaniculata* and *Hedyotiscorymbosa* extracts and their combination with curcumin. *Malar. J.* **2009**, *8*, 26.
(9) Radhika, P.; Lakshmi, K. R. Antimicrobial activity of the chloroform extracts of the root and the stem of *Andrographispaniculatanees*. *Int Res J Microbiol* **2010**, *1*, 037−039.
(10) Roy, S.; Rao, K.; Bhuvaneswari, C. H.; Giri, A.; Mangamoori, L. N. Phytochemical analysis of *Andrographispaniculata* extract and its antimicrobial activity. *World J. Microbiol. Biotechnol.* **2010**, *26*, 85.
(11) Kleipool, R. J. C. Constituents of *Andrographispaniculata* Nees. *Nature* **1952**, *169*, 33−34.
(12) Chan, W. R.; Taylor, D. R.; Willis, C. R.; Bodden, R. L.; Fehlhaber, H. W. The structure and stereochemistry of neoandrographolide, a diterpeneglucoside from *Andrographispaniculata* Nees. *Tetrahedron* **1971**, *27*, 5081−5091.
(13) Li, Y.; Lin, H. X.; Wang, J.; Yang, J.; Lai, C. J.; Wang, X.; Ma, B. W.; Tang, J. F.; Li, Y.; Li, X. L.; Guo, J. Glucosyltransferase Capable of Catalyzing the Last Step in Neoandrographolide Biosynthesis. *Org. Lett.* **2018**, *20*, 5999−6002.
(14) Rahman, N. N. N. A.; Furuta, T.; Takane, K.; Mohd, M. A. Antimalarial activity of extracts of Malaysian medicinal plants. *J. Ethnopharmacol.* **1999**, *64*, 249−254.
(15) Sharma, V.; Kapoor, K. K.; Mukherjee, D.; Gupta, V. K.; Dhar, M. K.; Kaul, S. Camphor sulphonic acid mediated quantitative 1, 3−diol protection of major Labdane diterpenes isolated from *Andrographis paniculata*. *Nat. Prod. Res.* **2018**, *32*, 1751−1759.
(16) Pfisterer, P.; Rollinger, J.; Schyschka, L.; Rudy, A.; Vollmar, A.; Stuppner, H. Neoandrographolide from *Andrographis* paniculata as a potential natural chemosensitizer. *Planta Med.* **2010**, *76*, 1698−1700.
(17) Xu, S.; Held, I.; Kempf, B.; Mayr, H.; Steglich, W.; Zipse, H. The DMAP-catalyzed acetylation of alcohols—A mechanistic study (DMAP= 4-(Dimethylamino) pyridine). *Chem.—Eur. J.* **2005**, *11*, 4751−4757.
(18) Boons, G. J.; Hale, K. J. *Organic Synthesis with Carbohydrates*; Wiley: United States, 2008; Vol. *1*, p 26.
(19) Vichai, V.; Kirtikara, K. Sulforhodamine B colorimetric assay for cytotoxicity screening. *Nat. Protoc.* **2006**, *1*, 1112−1116.
(20) Afsar, T.; Trembley, J. H.; Salomon, C. E.; Razak, S.; Khan, M. R.; Ahmed, K. Growth inhibition and apoptosis in cancer cells induced by polyphenolic compounds of *Acacia hydaspica*: involvement of multiple signal transduction pathways. *Sci. Rep.* **2016**, *6*, 23077.
(21) Wang, H.; Gao, Z.; Agarwal, P.; Zhao, S.; Conroy, D. W.; Ji, G.; Yu, J.; Jaroniec, C. P.; Liu, Z.; Lu, X.; Li, X. Overcoming ovarian cancer drug resistance with a cold responsive nanomaterial. *ACS Cent. Sci.* **2018**, *4*, 567−581.
(22) Larsen, A. K.; Hall, A.; Lundsgart, H.; Moghimi, S. M. Combined fluorimetric caspase 3/7 assay and bradford protein determination for assessment of polycation-mediated cytotoxicity. *Methods Mol. Biol.* **2013**, *948*, 23−33.
(23) Cao, P.; Xia, Y.; He, W.; Zhang, T.; Hong, L.; Zheng, P.; Shen, X.; Liang, G.; Cui, R.; Zou, P. Enhancement of oxaliplatin-induced colon cancer cell apoptosis by alantolactone, a natural product inducer of ROS. *Int. J. Biol. Sci.* **2019**, *15*, 1676−1684.
(24) Yang, B.; Johnson, T. S.; Thomas, G. L.; Watson, P. F.; Wagner, B.; Furness, P. N.; El Nahas, A. M. A shift in the Bax/Bcl-2 balance may activate caspase-3 and modulate apoptosis in experimental glomerulonephritis. *Kidney Int.* **2002**, *62*, 1301−1313.

DOI: 10.1021/acsomega.9b01249
ACS Omega 2019, 4, 20435−20442